



Kinetic modeling of azo dyes photocatalytic degradation in aqueous TiO₂ suspensions. Toxicity and biodegradability evaluation

María L. Satuf*, María J. Pierrestegui, Lorena Rossini, Rodolfo J. Brandi, Orlando M. Alfano

INTEC - Universidad Nacional del Litoral and CONICET, Güemes 3450, S3000GLN Santa Fe, Argentina

ARTICLE INFO

Article history:

Received 15 June 2010
Received in revised form
22 September 2010
Accepted 7 November 2010
Available online 10 December 2010

Keywords:

Azo dyes
Photocatalysis
Kinetics
Reactor modeling
Biodegradability
Toxicity

ABSTRACT

A kinetic model of the photocatalytic degradation of the azo dye Acid Orange 7 (AO7) is presented. It is based on mechanistic reaction steps and includes the modeling of the radiation absorption effects. The evaluation of the radiation field inside the reactor was achieved by solving the radiative transfer equation for the heterogeneous system. The study was carried out in a slurry batch photoreactor with recycle, employing artificial UV light as the source of radiation and TiO₂ Degussa P25 as catalyst. The biodegradability and toxicity of the irradiated mixture was also assessed. The kinetic model satisfactorily represents the evolution of AO7 under different experimental conditions, with a root mean square error of the estimations of 13.9%. The biodegradability of the AO7 solution was considerably enhanced after the photocatalytic treatment. In addition, a clear reduction of the toxicity of the azo dye was achieved at the end of the experiments.

© 2010 Elsevier B.V. All rights reserved.

1. Introduction

Wastewaters from the textile industry contain large amounts of organic dyes, representing a major threat to the environment due to their toxicity and potentially carcinogenic nature [1]. Azo dyes represent the most significant group of dyes used in the textile industry today [2]. Traditional physical treatment methods, like adsorption on activated carbon or ultrafiltration, can be applied to remove this kind of organic compounds from wastewaters but, as they are non-destructive, they just transfer the pollutants from water to another phase and originate the problem of secondary pollution. Besides, biological methods result ineffective to degrade azo dyes due to their resistant to biodegradation [3]. Therefore, advanced oxidation processes (AOPs) appear as effective alternative methods to treat textile effluents. The main advantage of these processes is that they can destroy organic molecules, leading to their complete mineralization or to biodegradable intermediate compounds. Among AOPs, heterogeneous photocatalysis with titanium dioxide (TiO₂) has been successfully applied to degrade organic dyes. Scientific research on the application of photocatalysis for textile effluents treatment has been revised in recent review papers [3,4]. Most studies deal with the degradation of dyes under different working conditions and are focused on the

factors that influence the reaction rate, but little information is provided on kinetic modeling based on mechanistic steps and including radiation absorption effects. Also, information concerning the evolution of toxicity and biodegradability of the treated samples is scarce [5,6]. The use of AOPs as a pre-treatment step to enhance the biodegradability of wastewaters can significantly reduce operational costs and increase the efficiency of the overall process. Therefore, determining the biodegradability and toxicity of intermediate species is a critical point in evaluating the possibility of photocatalysis to be employed as a pre-treatment process [7,8].

Reactor modeling involving the evaluation of the radiation field is essential to obtain intrinsic kinetic expressions that can be used for the design and optimization of photocatalytic devices. In the present work, we propose an intrinsic kinetic expression to represent the photocatalytic degradation rate of the azo dye Acid Orange 7 (AO7). It is based on mechanistic reaction steps and includes the modeling of the radiation absorption effects. The evaluation of the radiation field inside the reactor was achieved by solving the radiative transfer equation (RTE) for the heterogeneous system, where absorption and scattering take place. The toxicity and biodegradability of the photodegradation products have been evaluated by employing the Microtox[®] acute toxicity test and the 5-days biochemical oxygen demand (BOD₅) assay, respectively. The study was carried out in a slurry batch photoreactor with recycle, employing artificial UV light as the source of radiation and TiO₂ Degussa P25 as catalyst.

* Corresponding author. Tel.: +54 342 451 1546; fax: +54 342 451 1087.
E-mail address: mlsatuf@santafe-conicet.gov.ar (M.L. Satuf).

Nomenclature

AO7	Acid Orange 7
a_v	catalytic surface area per unit suspension volume (cm^{-1})
BOD	biochemical oxygen demand ($\text{mg O}_2 \text{ L}^{-1}$)
C	molar concentration in the suspension bulk (mol cm^{-3})
C_m	catalyst mass concentration (g cm^{-3})
COD	chemical oxygen demand ($\text{mg O}_2 \text{ L}^{-1}$)
e^a	local volumetric rate of photon absorption (Einstein $\text{cm}^{-3} \text{ s}^{-1}$)
g	asymmetry factor (dimensionless)
I	radiation intensity (Einstein $\text{cm}^{-2} \text{ sr}^{-1} \text{ s}^{-1}$)
K	equilibrium adsorption constant ($\text{cm}^3 \text{ mol}^{-1}$)
k	kinetic constant ($\text{cm}^2 \text{ mol}^{-1} \text{ s}^{-1}$)
p	phase function (dimensionless)
Q_L	irradiation level (%)
RMSE	root mean square error (%)
r	superficial reaction rate ($\text{mol cm}^{-2} \text{ s}^{-1}$)
r_{gs}	superficial rate of electron-hole generation ($\text{mol cm}^{-2} \text{ s}^{-1}$)
S_g	catalyst specific surface area ($\text{cm}^2 \text{ g}^{-1}$)
TOC	total organic carbon (mg L^{-1})
t	time (s)
V	volume (cm^3)
X_i	organic intermediates
x	axial coordinate (cm)
x	position vector (cm)
Y_i	inorganic radicals and species

Greek letters

α_i	kinetic parameter
ε_L	liquid hold-up (dimensionless)
β	volumetric extinction coefficient (cm^{-1})
β^*	specific extinction coefficient ($\text{cm}^2 \text{ g}^{-1}$)
Γ_W	global reflection coefficient of the reactor windows (dimensionless)
θ	spherical coordinate (rad)
θ_c	critical angle (rad)
κ	volumetric absorption coefficient (cm^{-1})
κ^*	specific absorption coefficient ($\text{cm}^2 \text{ g}^{-1}$)
μ	direction cosine of the ray for which the RTE is written
μ'	direction cosine of an arbitrary ray before scattering
μ_0	cosine of the angle between the direction of the incident and the scattered rays
μ_c	cosine of the critical angle θ_c
σ	volumetric scattering coefficient (cm^{-1})
σ^*	specific scattering coefficient ($\text{cm}^2 \text{ g}^{-1}$)
$\bar{\phi}$	wavelength averaged primary quantum yield (mol Einstein^{-1})

Subscripts

ads	adsorbed on the catalyst surface
A_R	catalytic reaction area
HG	Henry and Greenstein
R	reactor
T	total
0	initial condition; also, relative to the reactor window at $x=0$
λ	dependence on wavelength

Special symbol

[]	concentration on the catalyst surface (mol cm^{-2})
-----	--

2. Material and methods

2.1. Chemicals

Acid Orange 7 (AO7, molecular formula $\text{C}_{16}\text{H}_{11}\text{N}_2\text{O}_4\text{SNa}$), obtained from Aldrich, was employed as the model pollutant. TiO_2 powder (Degussa P25, ca. 80% anatase and 20% rutile, specific surface area $50 \text{ m}^2 \text{ g}^{-1}$) was used as photocatalyst. All solutions were prepared with deionized and doubly distilled water.

2.2. Experimental setup and procedure

The study was carried out in a batch photoreactor with recycle. A scheme of the experimental device is presented in Fig. 1. The reactor was cylindrical, made of glass, with a length of 10.4 cm and a diameter of 5.5 cm. It had a circular, flat window made of borosilicate glass. The illuminated surface was 23.8 cm^2 . The reactor volume was 274 cm^3 and the total volume of the system (V_T) was 1000 cm^3 . Radiation was provided by a CLEO HPA lamp (400 W from Philips) with emission in the UV and visible range, situated at the focal axis of a parabolic reflector. A filter containing a refrigerated solution of CoSO_4 was placed between the reactor and the lamp to avoid infrared and visible radiation. The resulting radiation arriving at the reactor window was comprised between 300 and 420 nm, with a peak at 370 nm. The storing tank was fitted with a sampling valve, a gas inlet for oxygen supply, and a water-circulating jacket to ensure isothermal conditions during the reaction time (293 K). A peristaltic pump (Masterflex[®]) was employed to recirculate the suspension in the system. The incident radiation flux at the reactor window, experimentally measured by ferrioxalate actinometry [9], was $7.45 \times 10^{-8} \text{ Einstein cm}^{-2} \text{ s}^{-1}$. Optical neutral filters were used to carry out experiments at different irradiation levels (Q_L). Also, a quartz ground plate was located at the reactor window to produce diffuse inlet radiation.

In a typical experiment, the reacting suspension comprised a defined amount of AO7 and TiO_2 dispersed in a total volume of 1000 cm^3 . All experiments were performed at natural pH (5.9). The suspension was sonicated during 30 min and then added to the tank. The reacting mixture, circulating at a flow rate of $100 \text{ cm}^3 \text{ s}^{-1}$, was saturated with pure oxygen by intense bubbling for 45 min. During this time interval, the lamp was turned on in order to reach stable operating conditions. A shutter located between the lamp and the reactor window prevented radiation to arrive at the reactor. Then, the initial sample was taken ($t=0$) and the shutter was removed to start the experimental run. The system was maintained under overpressure of oxygen to guarantee the renewal of the oxygen consumed by the photocatalytic reaction. At regular time intervals, samples were taken, centrifuged and filtered through a $0.02 \mu\text{m}$ syringe filter (Anotop 25) to remove the catalyst particles before analysis.

A control experiment was carried out to evaluate direct photolysis. The experiment was conducted following the procedure indicated above but without the addition of TiO_2 . No detectable changes occurred in the concentration of AO7 after 5 h of irradiation. Additionally, dark control experiments to assess adsorption of the dye have been performed. Adsorption equilibrium was obtained after 45 min of contact between the dye and TiO_2 (no modifications in the bulk concentration of the dye was detected after this time interval). Therefore, the reacting mixture was recirculated in the reactor for 45 min before the beginning of the illuminated reaction.

Experimental runs were performed at different AO7 initial concentrations ($C_{\text{AO7},0} = 2.7\text{--}11.0 \times 10^{-8} \text{ mol cm}^{-3}$), catalyst loadings ($C_m = 0.25, 0.5, 1.0 \text{ g L}^{-1}$), and levels of UV irradiation ($Q_L = 31.5, 74.2, 100\%$).

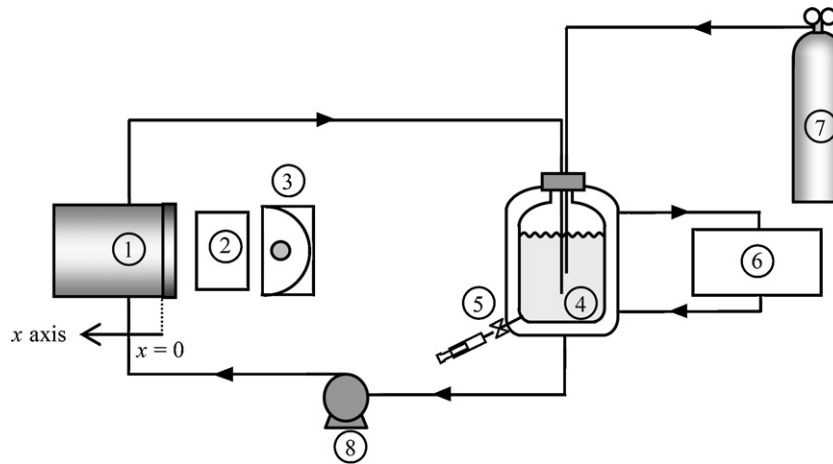


Fig. 1. Schematic representation of the experimental setup: 1, reactor; 2, CoSO₄ filter; 3, lamp; 4, tank; 5, sampling valve; 6, thermostatic bath; 7, oxygen supply; and 8, pump.

2.3. Analysis

The concentration of AO7 was measured by HPLC and visible spectroscopy. HPLC analysis with UV detection was performed using a Waters chromatograph equipped with a LC-18 Supelcosil reversed phase column (Supelco). The eluent was a binary mixture of acetonitrile and aqueous solution of ammonium acetate (10 mM) 24:76 (v/v), pumped at a rate of 1.5 cm³ min⁻¹. UV-vis absorption spectra of the samples were acquired in a Cary 100 Bio UV-visible spectrophotometer, over the range 200–600 nm. The absorbance at 484 nm was employed to quantify AO7. The mineralization of the pollutant was assessed by total organic carbon (TOC) analysis, employing a Shimadzu TOC-5000 A analyzer. The chemical oxygen demand (COD) measurements were obtained by following the closed reflux, colorimetric method [10]. The 5-days biochemical oxygen demand assay (BOD₅) was employed to evaluate changes in the biodegradability of the samples, employing the respirometric method [10] with a BOD System (Velp Scientifica) and PolySeed[®] inoculum (Interlab[®]). The toxicity evolution of the reacting mixture was assessed by the Microtox[®] acute toxicity test with *V. fischeri* using a Model 500 Analyzer (Strategic Diagnostics Inc.), according to ASTM Standard Method D 5660-96 [11].

3. Theory

3.1. Mass balance

The mass balance of AO7 was solved in order to obtain the theoretical evolution of the pollutant. To accomplish this, a number of assumptions were made: (i) there is a differential conversion per pass in the reactor, (ii) the system is perfectly stirred, (iii) there are no mass transport limitations, (iv) the chemical reaction occurs only at the solid–liquid interface [12,13], and (v) direct photolysis is neglected. As a result, the mass balance for AO7 in the system takes the following form [14]:

$$\varepsilon_L \frac{dC_{AO7}(t)}{dt} = -\frac{V_R}{V_T} a_v \langle r_{AO7}(\mathbf{x}, t) \rangle_{A_R} \quad C_{AO7}(t=0) = C_{AO7,0} \quad (1)$$

where ε_L is the liquid hold-up ($\varepsilon_L \cong 1$), C_{AO7} is the molar concentration of AO7, t denotes reaction time, V_R is the reactor volume, V_T is the total system volume, a_v denotes the catalytic surface area per unit suspension volume, and $\langle r_{AO7}(\mathbf{x}, t) \rangle_{A_R}$ is the superficial reaction rate averaged over the catalytic reaction area A_R . The value of

Table 1

Reaction scheme for the photocatalytic degradation of AO7.

Step	Reaction	Rate
Activation	$TiO_2 + h\nu \rightarrow TiO_2 + e^- + h^+$	r_{gs}
Recombination	$e^- + h^+ \rightarrow \text{heat}$	$k_2[e^-][h^+]$
Electron trapping	$e^- + O_{2,ads} \rightarrow \bullet O_2^-$	$k_3[e^-][O_{2,ads}]$
Hole trapping	$h^+ + H_2O_{ads} \rightarrow \bullet OH + H^+$ $h^+ + OH^- \rightarrow \bullet OH$	$k_4[h^+][H_2O_{ads}]$
Hydroxyl attack	$AO7_{ads} + \bullet OH \rightarrow X_i$ $Y_{i,ads} + \bullet OH \rightarrow Y_m$	$k_5[\bullet OH][AO7_{ads}]$ $k'_1[\bullet OH][Y_{i,ads}]$
Adsorption	$site_{O_2} + O_2 \leftrightarrow O_{2,ads}$ $site_{H_2O} + H_2O \leftrightarrow H_2O_{ads}$ $site_{H_2O} + H_2O \leftrightarrow OH^- + H^+$ $site_{AO7} + AO7 \leftrightarrow AO7_{ads}$ $site_{AO7} + X_i \leftrightarrow X_{i,ads}$ $site_{Y_1} + Y_1 \leftrightarrow Y_{1,ads}$	

a_v , is computed from the product of the catalyst specific surface area (S_g) and the catalyst loading (C_m).

3.2. Kinetic model

The kinetic model proposed for the photocatalytic degradation of AO7 is based on the reaction scheme summarized in Table 1 [15,16], where X_i represents the organic intermediates of the reaction and Y_1 represents inorganic species that compete with the organic substrate for OH \cdot . The kinetic model assumes that photocatalytic reactions occur at the surface of the catalyst particles among adsorbed species [13], and that dynamic equilibrium is achieved between bulk and adsorbed concentrations of water, oxygen, organic compounds, and inorganic species [16,17]. Molecular oxygen and organic compounds are considered to adsorb on different sites of the TiO₂ particle [18]. Although adsorption sites for the organics are assumed to be the same, no important amounts of aromatic intermediates were detected under our experimental conditions (see Section 4). Therefore, the competition for adsorption sites between AO7 and the organic intermediates can be neglected.

Taking into account the above considerations, the following equations can be written:

$$[AO7_{ads}] = K_{AO7}[site_{AO7}]C_{AO7} \quad (2)$$

$$[O_{2,ads}] = K_{O_2}[site_{O_2}]C_{O_2} \quad (3)$$

where $[AO7_{ads}]$ and $[O_{2,ads}]$ represents the concentration of AO7 and O₂, respectively, adsorbed at the catalyst surface, K_j are the

equilibrium adsorption constants, $[\text{site}_i]$ represents the superficial concentration of vacant adsorption sites, and C_j are the concentration of AO7 and O_2 in the suspension bulk.

By making a balance of sites and employing the above equations, it is possible to relate the concentration of vacant sites to the total concentration of sites, $[\text{site}_{j,T}]$:

$$[\text{site}_{\text{AO7}}] = \frac{[\text{site}_{\text{AO7},T}]}{1 + K_{\text{AO7}}C_{\text{AO7}}} \quad (4)$$

$$[\text{site}_{\text{O}_2}] = \frac{[\text{site}_{\text{O}_2,T}]}{1 + K_{\text{O}_2}C_{\text{O}_2}} \quad (5)$$

Considering that the hydroxyl radical attack is the main route for the degradation of the model pollutant, the superficial degradation rate of AO7 can be represented by

$$r_{\text{AO7}} = k_5[\bullet\text{OH}][\text{AO7}_{\text{ads}}] \quad (6)$$

where k_5 is the kinetic constant of the reaction between the AO7 and hydroxyl radicals, and $[\bullet\text{OH}]$ is the concentration of hydroxyl radicals at the surface of the TiO_2 particles.

By applying the kinetic micro steady state approximation for the concentration of electrons, holes and hydroxyl radicals [15], we obtain the following expressions:

$$r_{e^-} = r_{\text{gs}} - k_2[e^-][h^+] - k_3[e^-][\text{O}_{2,\text{ads}}] \approx 0 \quad (7)$$

$$r_{h^+} = r_{\text{gs}} - k_2[e^-][h^+] - k_4[h^+][\text{H}_2\text{O}_{\text{ads}}] \approx 0 \quad (8)$$

$$r_{\bullet\text{OH}} = k_4[h^+][\text{H}_2\text{O}_{\text{ads}}] - k_5[\bullet\text{OH}][\text{AO7}_{\text{ads}}] - \sum_l k_l'[\bullet\text{OH}][Y_{l,\text{ads}}] \approx 0 \quad (9)$$

where r_{e^-} , r_{h^+} , and $r_{\bullet\text{OH}}$ correspond to the reaction rate of electrons, holes and hydroxyl radicals, respectively. Introducing $[e^-]$ from Eq. (7) into Eq. (8) and solving the quadratic equation, the expression for the hole concentration is obtained:

$$[h^+] = \left\{ -1 + \left(1 + \frac{4r_{\text{gs}}k_2}{k_4k_3[\text{H}_2\text{O}_{\text{ads}}][\text{O}_{2,\text{ads}}]} \right)^{1/2} \right\} \frac{k_3[\text{O}_{2,\text{ads}}]}{2k_2} \quad (10)$$

Then, introducing Eq. (10) into Eq. (9), taking out $[\bullet\text{OH}]$, and introducing it into Eq. (6), we arrive to the following equation:

$$r_{\text{AO7}} = \frac{k_5k_4k_3[\text{H}_2\text{O}_{\text{ads}}][\text{O}_{2,\text{ads}}][\text{AO7}_{\text{ads}}] \left\{ -1 + \left(1 + \frac{4r_{\text{gs}}k_2}{k_4k_3[\text{H}_2\text{O}_{\text{ads}}][\text{O}_{2,\text{ads}}]} \right)^{1/2} \right\}}{2k_2 \left\{ k_5[\text{AO7}_{\text{ads}}] + \sum_l k_l' [Y_{l,\text{ads}}] \right\}} \quad (11)$$

Two additional assumptions have been made to simplify the model [15,16,19]: (i) oxygen concentration is constant and in excess with respect to the stoichiometric demand, and (ii) the concentration of water molecules and hydroxyl ions on the catalytic surface remains constant.

Introducing Eq. (4), that represents the concentration of vacant sites for AO7, into Eq. (2), and introducing the resulting expression for $[\text{AO7}_{\text{ads}}]$ into Eq. (11), results:

$$r_{\text{AO7}} = \frac{\delta_2[\text{site}_{\text{AO7},T}]K_{\text{AO7}}C_{\text{AO7}}\{-1 + (1 + \delta_1r_{\text{gs}})^{1/2}\}}{C_{\text{AO7}}\{\delta_3K_{\text{AO7}} + K_{\text{AO7}}\} + 1} \quad (12)$$

where

$$\delta_1 = \frac{4k_2}{k_4k_3[\text{H}_2\text{O}_{\text{ads}}][\text{O}_{2,\text{ads}}]} \quad (13)$$

$$\delta_2 = \frac{k_5k_4k_3[\text{H}_2\text{O}_{\text{ads}}][\text{O}_{2,\text{ads}}]}{2k_2 \left(\sum_l k_l' [Y_{l,\text{ads}}] \right)} \quad (14)$$

$$\delta_3 = \frac{k_5}{\sum_l k_l' [Y_{l,\text{ads}}]} \quad (15)$$

The superficial rate of electron–hole generation, r_{gs} , is given by [19]:

$$r_{\text{gs}}(\mathbf{x}) = \frac{\bar{\phi}}{a_v} \int_{\lambda} e_{\lambda}^a(\mathbf{x}) d\lambda \quad (16)$$

where e_{λ}^a represents the local volumetric rate of photon absorption and $\bar{\phi}$ is the primary quantum yield averaged over the wavelength range.

Finally, introducing Eq. (16) into Eq. (12), and defining $e^a = \int_{\lambda} e_{\lambda}^a d\lambda$, we obtain:

$$r_{\text{AO7}}(\mathbf{x}, t) = \frac{\alpha_2 C_{\text{AO7}}(\mathbf{x}, t) \{-1 + [1 + \alpha_1 e^a(\mathbf{x}, t)/a_v]^{1/2}\}}{\alpha_3 C_{\text{AO7}}(\mathbf{x}, t) + 1} \quad (17)$$

where α_1 , α_2 and α_3 are the following kinetic parameters:

$$\alpha_1 = \delta_1 \bar{\phi} \quad (18)$$

$$\alpha_2 = \delta_2 [\text{site}_{\text{AO7},T}] K_{\text{AO7}} \quad (19)$$

$$\alpha_3 = [\text{site}_{\text{AO7},T}] \delta_3 K_{\text{AO7}} + K_{\text{AO7}} \quad (20)$$

3.3. Radiation model

As photocatalytic reactions start with the activation of TiO_2 by photon absorption, the knowledge of the radiation field inside the reactor is essential to model the kinetics of photocatalytic systems. The main changes in the spatial distribution of radiation inside the employed reactor occur along the x coordinate axis (Fig. 1), due to the extinction produced by the catalyst particles. This effect allows us to model the radiation propagation with only one spatial variable (x). Also, the arrangement of the lamp and the ground glass plate ensure the arrival of diffuse radiation with azimuthal symmetry at the reactor window. Consequently, radiation can be modeled with one angular variable (θ) [20]. The one-dimensional, one-directional radiation transport model, applied to solve the RTE in the photocatalytic reactor, yields [21]

$$\mu \frac{\partial I_{\lambda}(x, \mu)}{\partial x} + \beta_{\lambda} I_{\lambda}(x, \mu) = \frac{\sigma_{\lambda}}{2} \int_{\mu'=-1}^1 I_{\lambda}(x, \mu') p(\mu, \mu') d\mu' \quad (21)$$

where I_{λ} is the spectral radiation intensity; λ represents the radiation wavelength; x , is the axial coordinate; β_{λ} the volumetric extinction coefficient; σ_{λ} , the volumetric scattering coefficient; μ , the direction cosine of the ray for which the RTE is written ($\mu = \cos \theta$); μ' , the cosine of an arbitrary ray before scattering; and p represents the phase function for scattering. The Henyey and Greenstein phase function ($p_{\text{HG},\lambda}$) was adopted to model the radiation scattering of the TiO_2 suspension [22]:

$$p_{\text{HG},\lambda}(\mu_0) = \frac{1 - g_{\lambda}^2}{(1 + g_{\lambda}^2 - 2g_{\lambda}\mu_0)^{3/2}} \quad (22)$$

where g_{λ} is a free parameter called the asymmetry factor, and μ_0 represents the cosine of the angle between the direction of the incident and the scattered rays. The knowledge of g_{λ} alone suffices to obtain solutions of multiple scattering problems with a high grade of accuracy, making the HG phase function ideal for calculations.

The effects of reflection, refraction and absorption of radiation at the reactor window were taken into account to obtain the boundary conditions for Eq. (21). At $x=0$ (Fig. 1), radiation intensities are the result of two contributions: (i) the transmitted portion of the radiation coming from the lamp ($I_{0,\lambda}$ at $x=0$), and (ii) the reflected portion of the radiation coming from the suspension ($\Gamma_{\text{W},\lambda} I_{\lambda}$, where $\Gamma_{\text{W},\lambda}$ is the global reflection coefficient of the reactor windows). As a consequence of refraction, the angular directions of the specific intensities that enter the reactor are limited by the

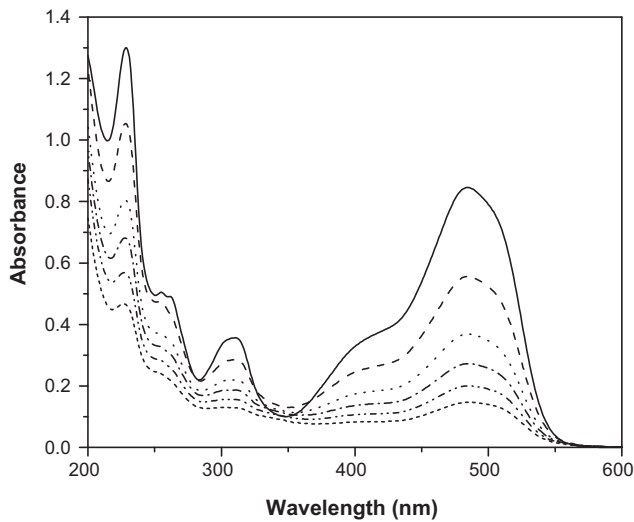


Fig. 2. UV spectra of the reacting mixture during a typical photocatalytic experiment: (—) $t=0$; (---) $t=1$ h; (.....) $t=2$ h; (- · - ·) $t=3$ h; (- - -) $t=4$ h; (- - - -) $t=5$ h.

critical angle of total reflection, θ_c . Then, the boundary conditions of the RTE result:

$$I_\lambda(0, \mu) = \Gamma_{W,\lambda}(-\mu)I_\lambda(0, -\mu) \quad 0 \leq \mu < \mu_c \quad (23)$$

$$I_\lambda(0, \mu) = I_{0,\lambda} + \Gamma_{W,\lambda}(-\mu)I_\lambda(0, -\mu) \quad \mu_c \leq \mu \leq 1 \quad (24)$$

where $\mu_c = \cos \theta_c$. More details concerning the radiation model can be found elsewhere [23].

The values of g_λ and the specific coefficients (per catalyst mass concentration C_m) β_λ^* and σ_λ^* employing the method described in a previous work [23]. The Discrete Ordinate Method [24] was applied to solve the radiation model. This method involves the spatial and directional discretization of the RTE, transforming Eq. (21) into a set of algebraic equations that can be solved numerically. The solution of the RTE provides the spectral radiation intensity at each point and each direction inside the reactor. Once the spectral intensities were obtained, the LVRPA, required to solve the reaction rate expression, was computed as:

$$e^a(x) = 2\pi \int_{\lambda} \kappa_\lambda \int_{\mu=-1}^1 I_\lambda(x, \mu) d\mu d\lambda \quad (25)$$

where κ_λ is the volumetric absorption coefficient.

4. Results and discussion

Fig. 2 presents the changes in the UV absorption spectra of the reacting solution at different irradiation times, for a typical run performed with $C_m = 1.0 \times 10^{-3} \text{ g cm}^{-3}$, $Q_L = 100\%$ and $C_{AO7,0} = 4.0 \times 10^{-8} \text{ mol cm}^{-3}$. At $t=0$, the spectrum is coincident with that of pure AO7, with two characteristic bands in the visible region at $\lambda = 430 \text{ nm}$ and $\lambda = 485 \text{ nm}$, corresponding to the azo form and hydrazone form of the dye, respectively, and two bands in the UV region at $\lambda = 228 \text{ nm}$ and $\lambda = 310 \text{ nm}$, attributed to the benzoic and naphthalene rings, respectively. As long as the reaction progresses, these bands decrease significantly without the appearance of new absorption peaks. The changes in TOC concentration were employed to estimate the mineralization of the organic compounds. At the end of the above mentioned experiment, although more than 80% conversion was achieved for AO7, TOC concentration was only reduced to ca. 27% of its initial value, indicating the presence of organic intermediates of the reaction. According to HPLC analysis, no important amounts of aromatic intermediates

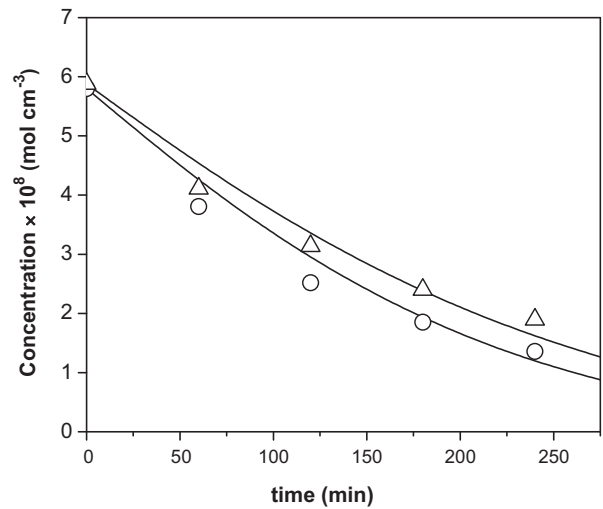


Fig. 3. Experimental and predicted concentrations of AO7 vs. time for $Q_L = 100\%$, $C_{AO7,0} = 6.0 \times 10^{-8} \text{ mol cm}^{-3}$ and different C_m . Experimental data: (○) $C_m = 1.0 \times 10^{-3} \text{ g cm}^{-3}$; (△) $C_m = 0.25 \times 10^{-3} \text{ g cm}^{-3}$. Model results: solid lines.

were detected under our experimental conditions after 5 h of irradiation. The contribution to the TOC concentration can therefore be attributed to low molecular weight compounds [1,25].

A Levenberg–Marquardt optimization algorithm was applied to estimate the kinetic parameters presented in Eq. (17). The experimental concentrations of AO7, obtained from samples at different reaction times, were compared with model results. The optimization procedure renders the values of the parameters that minimize the differences between predicted concentrations and experimental data. From the results of the optimization algorithm it was found that, under the operating conditions of the experiments, the term $\alpha_1 e^a(\mathbf{x}, \mathbf{t})/a_v$ was at least five orders of magnitude higher than 1. As a result, the term in braces in Eq. (17) can be simplified to $[\alpha_1 e^a(\mathbf{x}, \mathbf{t})/a_v]^{1/2}$, and the reaction rate equation takes the following form:

$$r_{AO7}(\mathbf{x}, \mathbf{t}) = \frac{\alpha C_{AO7}(\mathbf{x}, \mathbf{t}) [e^a(\mathbf{x}, \mathbf{t})/a_v]^{1/2}}{\alpha_3 C_{AO7}(\mathbf{x}, \mathbf{t}) + 1} \quad (26)$$

where $\alpha = \alpha_2(\alpha_1)^{1/2}$. The final values of the kinetic parameters, with the corresponding 95% confidence interval, are $\alpha = 2.37 (\pm 0.30) \text{ cm}^2 \text{ s}^{-1/2} \text{ Einstein}^{-1/2}$; $\alpha_3 = 1.79 (\pm 0.50) \times 10^7 \text{ cm}^3 \text{ mol}^{-1}$.

Figs. 3–5 depict the experimental and predicted concentrations of AO7 under different operating conditions. Symbols correspond to experimental data. Model predictions, represented by solid lines, were calculated by employing Eqs. (1) and (26) with the corresponding kinetic parameters. It can be observed that the degradation is enhanced by the increase in the TiO_2 loading and irradiation level. Considering all the runs, good agreement was obtained between model predictions and experimental data. The root mean square error (RMSE) of the estimations was computed as $\text{RMSE} = [1/N \sum_{i=1}^N C_{i,\text{exp}} - C_i/C_{i,\text{exp}}]^2]^{1/2} \times 100$, where $C_{i,\text{exp}}$ and C_i are the experimental and model concentrations of AO7, respectively, and N is the total number of samples for the complete set of experimental runs. The values of concentration lower than $1.0 \times 10^{-8} \text{ mol cm}^{-3}$ were excluded from calculations because they were comprised in the range of instrumental error. The RMSE was 13.9%.

The evolution of the biodegradability and toxicity of the treated solution is presented in Table 2, along with the AO7 and TOC conversion, for an experiment carried out with $C_m = 0.5 \times 10^{-3} \text{ g cm}^{-3}$, $Q_L = 100\%$ and $C_{AO7,0} = 2.9 \times 10^{-8} \text{ mol cm}^{-3}$. The biodegradability is expressed in terms of the BOD_5/COD ratio and the toxicity of

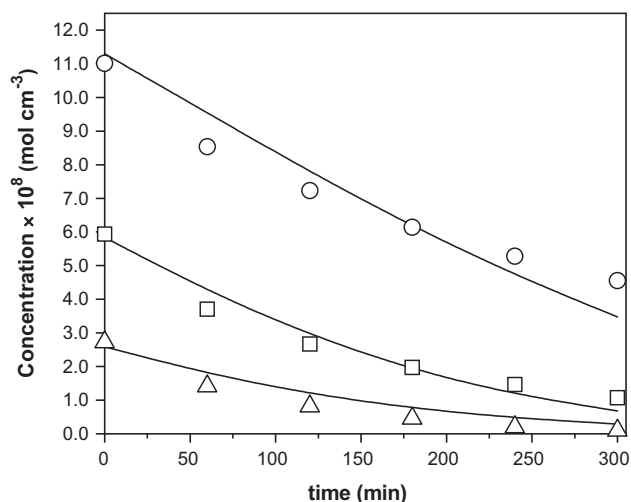


Fig. 4. Experimental and predicted concentrations of AO7 vs. time for $C_m = 0.5 \times 10^{-3} \text{ g cm}^{-3}$ and different $C_{AO7,0}$. Experimental data: (○) $C_{AO7,0} = 11.0 \times 10^{-8} \text{ mol cm}^{-3}$; (□) $C_{AO7,0} = 6.0 \times 10^{-8} \text{ mol cm}^{-3}$; (△) $C_{AO7,0} = 2.7 \times 10^{-8} \text{ mol cm}^{-3}$. Model results: solid lines.

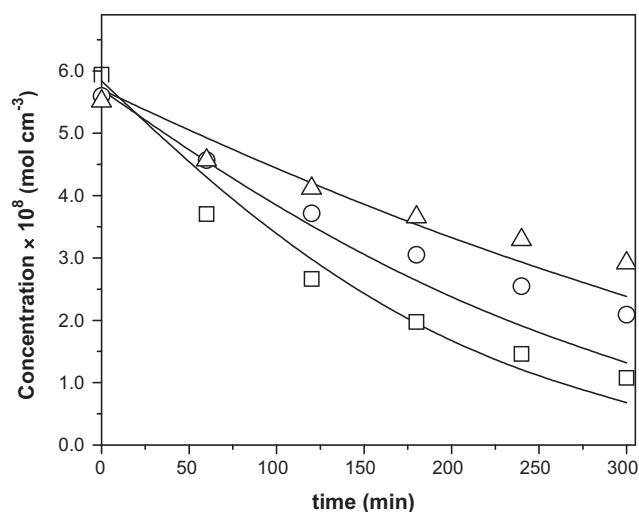


Fig. 5. Experimental and predicted concentrations of AO7 vs. time for $C_m = 0.5 \times 10^{-3} \text{ g cm}^{-3}$ and different Q_L . Experimental data: (□) $Q_L = 100\%$; (○) $Q_L = 74.2\%$; (△) $Q_L = 31.5\%$. Model results: solid lines.

the samples is represented by the percentage of inhibition of the natural bioluminescence of *Vibrio fischeri*. The initial solution is totally refractory to biodegradation and causes an inhibitory effect of almost 50%. As the treatment progresses, the biodegradability is enhanced and the toxicity diminishes. After 6 h, the solution reaches a BOD₅/COD ratio of 1.1. Taking into account that pollutants with a BOD₅/COD ratio between 0.4 and 0.8 can be considered biodegradable [5], the intermediate products of the reaction would be easily degradable by microorganisms in a successive biological treatment. Regarding toxicity effects, by the end of the photodegradation, inhibition represents only 8.6%. It should be marked that

Table 2
Biodegradability and toxicity evolution.

Reaction time	0 min	180 min	360 min
AO7 conversion (%)	0.0	50.5	94.3
TOC conversion (%)	0.0	39.3	44.1
BOD ₅ /COD	0.0	0.6	1.1
Inhibition (%)	47.7	43.9	8.6

more than 50% of the initial TOC content of the sample still remains after 360 min. From these results we can conclude that it is not necessary to completely mineralize the azo dye solution because intermediate organic compounds present after 360 min of treatment are easily biodegradable and present very low toxicity values.

5. Conclusions

The modeling of a photocatalytic slurry reactor for the degradation of the azo dye AO7 is presented. The reactor model includes explicitly the effect of radiation absorption on the reaction rate. Good fitting of experimental data was obtained with only two kinetic parameters, with a root mean square error of the estimations of 13.9%. The toxicity and biodegradability of the reacting mixture was also evaluated. The Microtox[®] assay indicated that the toxicity of the pollutant was significantly reduced after the treatment. Additionally, the photocatalytic process clearly enhanced the biodegradability of the samples. Consequently, this AOP could be used as a pre-treatment method to degrade bio-recalcitrant organic dyes.

Acknowledgments

The authors are grateful to Universidad Nacional del Litoral (UNL), Consejo Nacional de Investigaciones Científicas y Técnicas (CONICET) and Agencia Nacional de Promoción Científica y Tecnológica (ANPCyT) for the financial support. They also thank Antonio C. Negro for his valuable help during the experimental work.

References

- [1] M. Styliadi, D.I. Kondarides, X.E. Verykios, *Appl. Catal. B* 40 (2003) 271–286.
- [2] H. Zollinger, *Color Chemistry: Synthesis Properties and Applications of Organic Dyes and Pigments*, VCH Publishers, New York, 1991.
- [3] I.K. Konstantinou, T.A. Albanis, *Appl. Catal. B* 49 (2004) 1–14.
- [4] S. Ahmed, M.G. Rasul, W.N. Martens, R. Brown, M.A. Hashib, *Water Air Soil Pollut.* (2010), doi:10.1007/s11270-010-0456-3.
- [5] F. Al-Momani, E. Touraud, J.R. Degorce-Dumans, J. Roussy, O. Thomas, *J. Photochem. Photobiol. A* 153 (2002) 191–197.
- [6] S. Brosillon, H. Djelal, N. Merienne, A. Amrane, *Desalination* 222 (2008) 331–339.
- [7] M. Lapertot, S. Ebrahimi, I. Oller, M.I. Maldonado, W. Gernjak, S. Malato, C. Pulgarín, *Ecotoxicol. Environ. Saf* 69 (2008) 546–555.
- [8] S. Malato, P. Fernández-Ibañez, M.I. Maldonado, J. Blanco, W. Gernjak, *Catal. Today* 147 (2009) 1–59.
- [9] S.L. Murov, I. Carmichael, G.L. Hug, *Handbook of Photochemistry*, 2nd ed., Marcel Dekker, New York, 1993.
- [10] *Standard Methods for the Examination of Water and Wastewater*, 20th ed., American Public Health Association/American Water Works Association/Water Environmental Federation, Washington, DC, 1998.
- [11] ASTM Standard D5660-96, Standard Test Method for Assessing the Microbial Detoxification of Chemically Contaminated Water and Soil Using a Toxicity Test with a Luminescent Marine Bacterium, ASTM International, West Conshohocken, PA, 2004, doi:10.1520/D5660-96R04, www.astm.org.
- [12] C. Minero, F. Catozzo, E. Pelizzetti, *Langmuir* 8 (1992) 481–486.
- [13] E. Pelizzetti, C. Minero, *Electrochim. Acta* 38 (1993) 47–55.
- [14] M.I. Cabrera, A.C. Negro, M. Alfano, A.E. Cassano, *J. Catal.* 172 (1997) 380–390.
- [15] C.S. Turchi, D.F. Ollis, *J. Catal.* 122 (1990) 178–192.
- [16] C.B. Almquist, P. Biswas, *Chem. Eng. Sci.* 56 (2001) 3421–3430.
- [17] M.F.J. Dijkstra, H.J. Panneman, J.G.M. Winkelman, J.J. Kelly, A.A.C.M. Beenackers, *Chem. Eng. Sci.* 57 (2002) 4895–4907.
- [18] R. Terzian, N. Serpone, C. Minero, E. Pelizzetti, H. Hidaka, *J. Photochem. Photobiol. A* 55 (1990) 243–249.
- [19] O.M. Alfano, M.I. Cabrera, A.E. Cassano, *J. Catal.* 172 (1997) 370–379.
- [20] M.N. Özışık, *Radiative Transfer and Interactions with Conduction and Convection*, Wiley, New York, 1973.
- [21] O.M. Alfano, A.C. Negro, M.I. Cabrera, A.E. Cassano, *Ind. Eng. Chem. Res.* 34 (1995) 488–499.
- [22] R. Siegel, J.R. Howell, *Thermal Radiation Heat Transfer*, 4th ed., Hemisphere Publishing Corp., Bristol, PA, 2002.
- [23] M.L. Satuf, R.J. Brandi, A.E. Cassano, O.M. Alfano, *Ind. Eng. Chem. Res.* 44 (2005) 6643–6649.
- [24] J.J. Duderstadt, W.R. Martin, *Transport Theory*, Wiley, New York, 1979.
- [25] M. Styliadi, D.I. Kondarides, X.E. Verykios, *Appl. Catal. B* 47 (2004) 189–201.